

Narrowing of Protein NMR Spectral Lines Broadened by Chemical Exchange

Ying Li and Arthur G. Palmer III*

Department of Biochemistry and Molecular Biophysics, Columbia University, New York, New York 10032

Received April 17, 2010; E-mail: agp6@columbia.edu

NMR techniques for characterizing chemical exchange phenomena have found widespread use in studies of protein and nucleic acid dynamics, which are closely linked to biological functions, including enzyme catalysis, ligand binding, and allosteric regulation.^{1,2} However, chemical exchange on microsecond to millisecond time scales broadens spectral lines, with deleterious effects on resolution and sensitivity. We present a multipulse method for reducing chemical exchange broadening during the frequency-encoding periods of liquid-state multidimensional NMR experiments. Enhanced resolution and sensitivity are demonstrated for exchange-broadened ¹⁵N resonances of the protein ribonuclease A (RNase A).

Transverse relaxation induced by chemical exchange depends on the kinetic rate constants of the chemical process and on the differences in resonance frequencies for nuclear spins in the interconverting molecular species. Kinetic rate constants are intrinsic physicochemical properties of a biological or chemical system, and manipulation of these properties is either difficult or undesirable. In contrast, isotropic chemical shifts can be partially refocused by radiofrequency (RF) pulse trains, as first demonstrated by Ellett and Waugh.³ This technique has been named “chemical shift scaling” (CSS) and is mainly used in solid-state NMR spectroscopy. Fluctuations in isotropic chemical shifts caused by chemical exchange also are reduced by CSS. If the kinetic process is in the fast-exchange limit and the cycle time of the RF pulses is much shorter than the kinetic time scale, then transverse relaxation is scaled by a factor σ^2 , in which the CSS factor is $0 < \sigma < 1$.⁴ The effective gain in resolution is $1/\sigma$ if loss from the scaled precession frequencies is taken into account and other relaxation mechanisms are not considered. If the kinetic process approaches the intermediate-to-slow exchange limits, then transverse relaxation is scaled by a factor that is larger than σ^2 and eventually reaches unity.

Zhuravleva and Orekhov⁵ recently applied a CSS scheme called “divided evolution” in liquid-state NMR experiments. This scheme alternates a free-precession period and a hard π -pulse train consisting of either 8 or 16 pulses applied with XY8 or XY16 phase cycles.⁶ Magnetization evolves in the transverse plane for nearly the entire divided-evolution trajectory. Therefore, the apparent transverse relaxation resulting from mechanisms other than chemical exchange is inflated by a factor of $1/\sigma$ and can contribute significantly to the total line widths, especially for large proteins. Practical use of the scheme also is hampered by the narrow spectral width that can be sampled without aliasing unless σ is very small, as a minimum spacing between hard pulses is required to avoid excessive heating.

To address these problems, we have implemented a four-pulse scheme based on the classical WAHUA⁷ and magic-echo^{8,9} sequences for homonuclear dipolar decoupling in solid-state NMR spectroscopy. Figure 1A shows the RF cycle of the proposed sequence with pulse phases and a set of optimal pulse flip angles. The four pulses are executed at low RF power to significantly shorten the RF cycle and therefore allow higher

sampling rates. Isotropic chemical shifts are scaled down by factors determined by the flip angles of the low-power pulses and the length of the flanking free-precession periods. To achieve the high degree of compensation for RF inhomogeneity required for high-resolution solution NMR applications, pulse flip angles and delays are optimized by numerical simulations performed with SPINEVOLUTION.¹⁰ Figure 1B shows the simulated line broadening as a function of resonance offsets for a Gaussian distribution of B_1 fields with a full width at half-height (fwhh) of 10%. Good compensation for RF inhomogeneity as well as uniform scaling factors can be achieved within an effective bandwidth of approximately ω_1 with the chosen set of parameters ($\tau_1 = 2\tau_{90}$, $\tau_2 = 0.03\tau_{90}$, and $\tau_3 = 0.5\tau_{90}$, where τ_{90} is the 90° pulse length), which gives $\sigma = 0.42$. Parameters for other scaling factors are included in the Supporting Information.

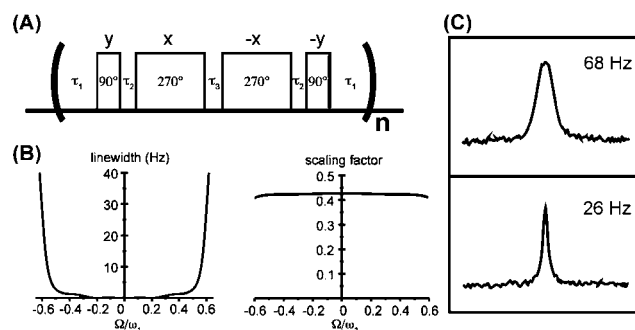


Figure 1. (A) RF cycle of the four-pulse scheme for chemical shift scaling. (B) Simulated line broadening by RF inhomogeneity and scaling factor as functions of the ratio of resonance offsets (Ω) to the B_1 field (ω_1) when $\tau_1 = 2\tau_{90}$, $\tau_2 = 0.03\tau_{90}$, and $\tau_3 = 0.5\tau_{90}$, where τ_{90} is the 90° pulse length. Line broadening is represented as the fwhh and is proportional to B_1 . A B_1 field of 2.5 kHz was used to produce the plot. (C) ¹³C lineshapes of [methyl-¹³C]DMTCA in the (top) direct and (bottom) indirect dimensions of a ¹³C–¹³C 2D spectrum with CSS applied to the t_1 evolution period. Both line shapes were extracted from a single diagonal peak. The parameters used for chemical shift scaling were $\tau_{90} = 60 \mu\text{s}$, $\tau_1 = 111 \mu\text{s}$, $\tau_2 = 10 \mu\text{s}$, and $\tau_3 = 38.4 \mu\text{s}$, and the scaling factor σ was 0.40.

The proposed sequence has more favorable relaxation properties than the divided-evolution scheme because the magnetization is placed along the z axis for part of the evolution trajectory, as previously demonstrated for TOCSY experiments.¹¹ During the four pulses, when they are executed without any interpulse delays, the effective relaxation rate is $0.5R_2^0 + 0.5R_1$ for x magnetization and $0.625R_2^0 + 0.375R_1$ for y magnetization, where R_2^0 represents the transverse relaxation rate constant for interactions other than chemical exchange and R_1 is the longitudinal relaxation rate constant. Relaxation during the entire RF cycle is further reduced by the shorter free-precession period needed to achieve a desired scaling factor because the chemical shifts are not completely refocused during the low-power RF pulses. As a practical advantage, sample heating also is reduced because the heating from RF pulses, when the flip angles are the same, is proportional to the B_1 field.

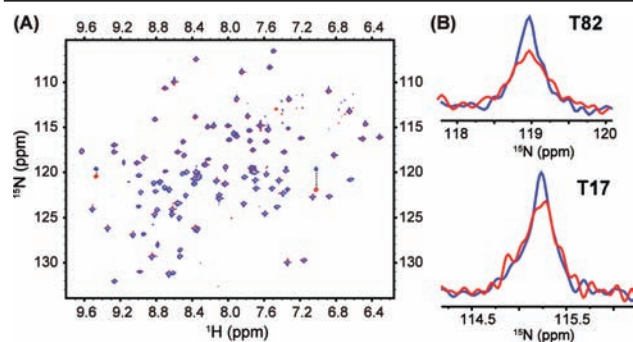


Figure 2. (A) Overlay of spectra for normal TROSY (red) and TROSY with CSS (blue) during the t_1 evolution period. Data were acquired for $[U\text{-}^2\text{H}, U\text{-}^{15}\text{N}]\text{RNase A}$ at 293 K on a Bruker DRX500 spectrometer equipped with a triple-resonance gradient probe. The parameters used for chemical shift scaling were $\tau_{90} = 100 \mu\text{s}$, $\tau_1 = 200 \mu\text{s}$, $\tau_2 = 3 \mu\text{s}$, $\tau_3 = 50 \mu\text{s}$, and $\sigma = 0.42$. Data were processed without apodization in the indirect dimensions. Cross-peaks connected by dotted lines belong to same residues and are outside the effective band width and also aliased. (B) ^{15}N line shapes of residues T82 and T17 in normal TROSY (red) and TROSY with CSS (blue).

The line-narrowing effects of the proposed scheme were confirmed by applying CSS during the t_1 evolution period of a ^{13}C – ^{13}C 2D experiment on the small molecule $[\text{methyl-}^{13}\text{C}_2]\text{N,N}$ -dimethyltrichloroacetamide (DMTCA), which contains two methyl groups in chemical exchange. For easy comparison of resolution, the spectral width of the indirect ^{13}C dimension was scaled by $1/\sigma$ to produce the same chemical shifts as the direct dimension. With a B_1 field much larger than the kinetic rate constant ($\sim 200 \text{ s}^{-1}$), the ^{13}C line width was reduced from 68 to 26 Hz (Figure 1C), consistent with the scaling factor $\sigma = 0.40$.

The proposed scheme was also validated using the protein $[U\text{-}^2\text{H}, U\text{-}^{15}\text{N}]\text{RNase A}$, which has been characterized previously by relaxation dispersion experiments.¹² CSS with $\sigma = 0.42$ was applied during the t_1 evolution period of a gradient-selected ^{15}N – ^1H TROSY sequence using a B_1 field of 2.5 kHz, resulting in an RF cycle time of ~ 1.3 ms; 202 complex points were collected in the t_1 dimension. For comparison, a normal TROSY spectrum was acquired with the same effective sampling rate and digital resolution. Figure 2A shows the overlay of the two spectra, illustrating uniform scaling factors across the entire spectral region. Six residues, whose original line widths ranged from 10 to 30 Hz, showed narrower lines under CSS. Figure 2B shows the ^{15}N line shapes for residues T82 and T17. T82 showed the most dramatic narrowing effects, with the line width being reduced from 30 to 19 Hz and the signal-to-noise ratio enhanced to 165% of the original. Resonances corresponding to residues not undergoing chemical exchange were broadened slightly. The average ^{15}N line width for all of the residues was 7.0 Hz in the normal TROSY experiment and 9.0 Hz in the TROSY experiment with CSS, consistent with good compensation for RF inhomogeneity. When chemical exchange broadening contributes to a larger fraction of the total line width than for RNase A, the experiment will benefit from choosing smaller scaling factors. TROSY experiments incorporating the divided-evolution scheme

were performed with the same $\sigma = 0.42$ and with $\sigma = 0.24$, nearly identical to that used by Zhuravleva and Orekhov.⁵ No reductions in line width were observed for any resonance in either experiment because of the less favorable relaxation properties and longer RF cycle and therefore slower averaging of chemical shifts.

In summary, we have presented a method based on chemical shift scaling for narrowing spectral lines severely broadened by chemical exchange. The favorable relaxation properties of the proposed scheme are especially suitable for proteins of high molecular weight. The method can be applied using RF powers available from current solution NMR probes, although higher powers would increase the effective band width and the range of exchange rates for which the technique is effective. CSS enhances the sensitivity of the most severely broadened lines and potentially allows detection of weak peaks that are below normal detection limits. CSS can also be combined with methods such as CPMG-INEPT^{13,14} or cross-polarization¹⁵ that reduce losses from chemical exchange during magnetization-transfer periods. Coherent averaging techniques, which were originally developed in solid-state NMR spectroscopy, are used widely for decoupling and isotropic mixing in liquid-state NMR experiments. The present work demonstrates additional applications for resolution enhancement in biological NMR spectroscopy.

Acknowledgment. This work was supported by National Institutes of Health Grant GM59273 (A.G.P.). We thank Eric Watt and J. Patrick Loria (Yale University) for providing the sample of RNase A. We thank Mark Rance (University of Cincinnati) for helpful discussions.

Supporting Information Available: Details of numerical optimization, a table containing pulse flip angles and delays for a range of σ values, additional experimental details, experimental data on ubiquitin, resonance offset dependence of σ , orientation of the effective magnetic field, effective relaxation rate, and dependence of the transverse relaxation rate from chemical exchange on B_1 field or pulsing rate. This material is available free of charge via the Internet at <http://pubs.acs.org>.

References

- (1) Boehr, D. D.; Dyson, H. J.; Wright, P. E. *Chem. Rev.* **2006**, *106*, 3055–3079.
- (2) Kern, D.; Zuiderweg, E. R. *Curr. Opin. Struct. Biol.* **2003**, *13*, 748–757.
- (3) Ellett, J. D.; Waugh, J. S. *J. Chem. Phys.* **1969**, *51*, 2851–2857.
- (4) Vega, A. J.; English, A. D.; Mahler, W. *J. Magn. Reson.* **1980**, *37*, 107–128.
- (5) Zhuravleva, A.; Orekhov, V. Y. *J. Am. Chem. Soc.* **2008**, *130*, 3260–3261.
- (6) Gullion, T.; Baker, D. B.; Conradi, M. S. *J. Magn. Reson.* **1990**, *89*, 479–484.
- (7) Waugh, J. S.; Huber, L. M.; Haeberle, U. *Phys. Rev. Lett.* **1968**, *20*, 180–182.
- (8) Takegoshi, K.; McDowell, C. A. *Chem. Phys. Lett.* **1985**, *116*, 100–104.
- (9) Boutis, G. S.; Cappellaro, P.; Cho, H.; Ramanathan, C.; Cory, D. G. *J. Magn. Reson.* **2003**, *161*, 132–137.
- (10) Veshort, M.; Griffin, R. G. *J. Magn. Reson.* **2006**, *178*, 248–282.
- (11) Bax, A.; Davis, D. G. *J. Magn. Reson.* **1985**, *65*, 355–360.
- (12) Cole, R.; Loria, J. P. *Biochemistry* **2002**, *41*, 6072–6081.
- (13) Mueller, L.; Legault, P.; Pardi, A. *J. Am. Chem. Soc.* **1995**, *117*, 11043–11048.
- (14) Mulder, F. A. A.; Spronk, C. A. E. M.; Slijper, M.; Kaptein, R.; Boelens, R. *J. Biomol. NMR* **1996**, *8*, 223–228.
- (15) Krishnan, V. V.; Rance, M. *J. Magn. Reson., Ser. A* **1995**, *116*, 97–106.

JA103251H